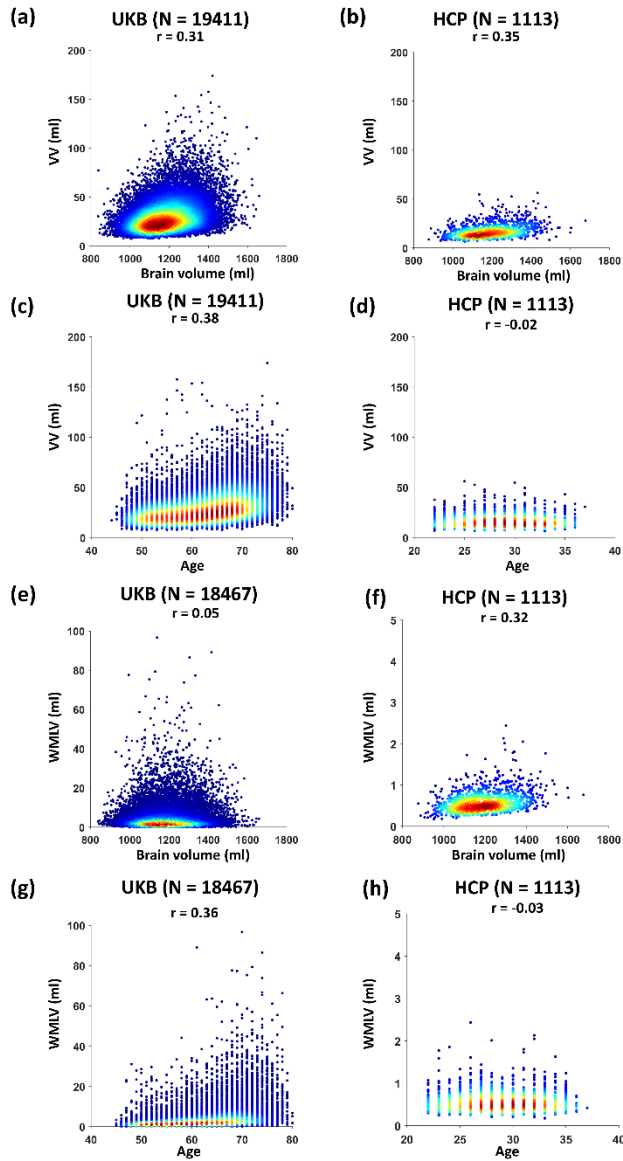
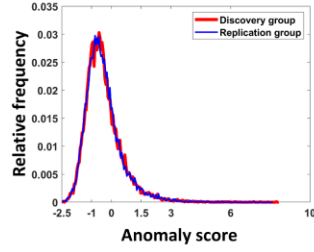


## Supplementary Information

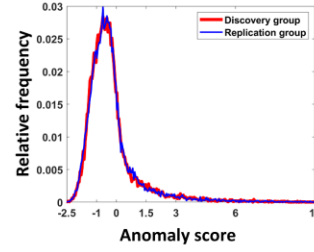


**Fig. S1.** The scatterplots between unidimensional imaging phenotypes (VV, WMLV; before covariate regression) and two covariates (brain volume, age). **(a)** Brain volume versus VV in the UKB cohort. **(b)** Brain volume versus VV in the HCP cohort. **(c)** Age versus VV in the UKB cohort. **(d)** Age versus VV in the HCP cohort. **(e)** Brain volume versus WMLV in the UKB cohort. **(f)** Brain volume versus WMLV in the HCP cohort. **(g)** Age versus WMLV in the UKB cohort. **(h)** Age versus WMLV in the HCP cohort.

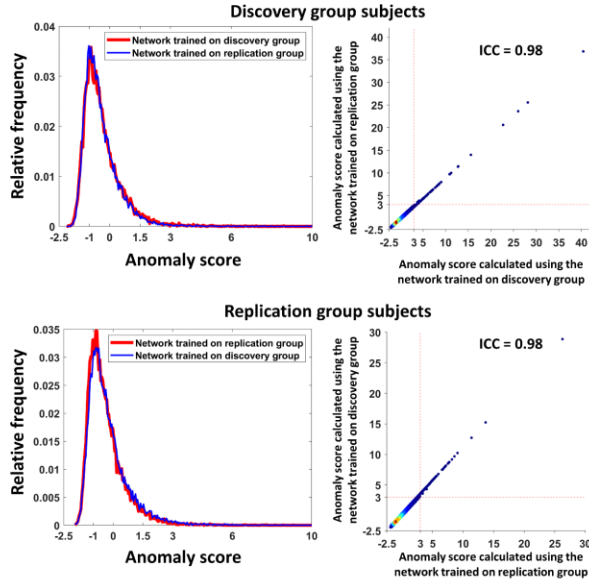
(a) VV



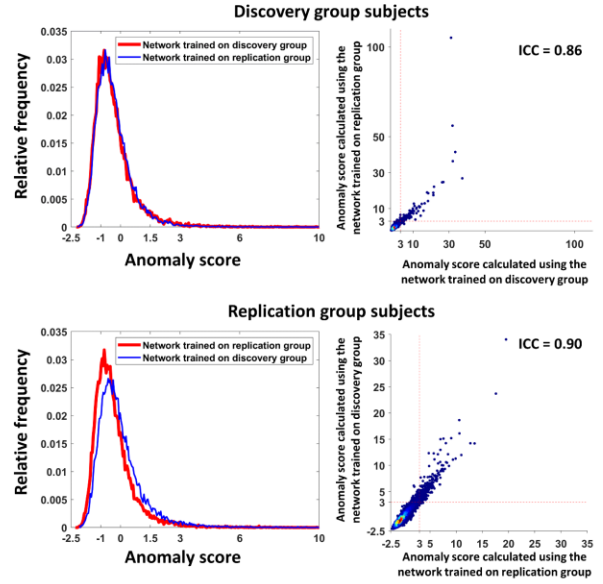
(b) WMLV



(c) FA



(d) MD



(e) CTh

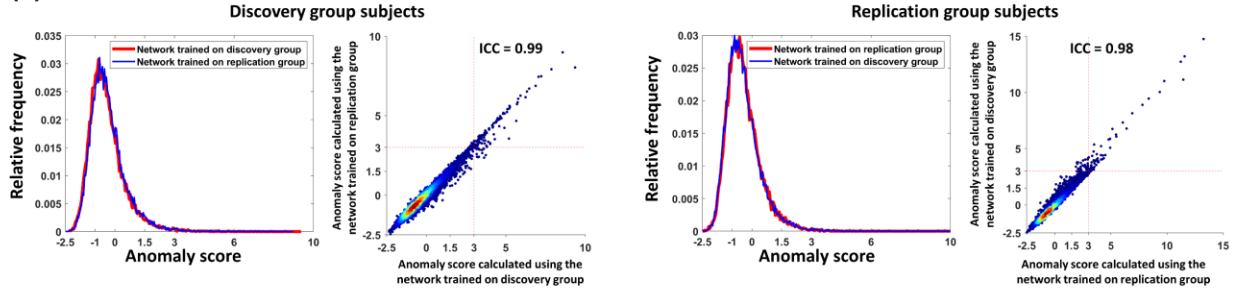


**Fig. S2.** Robustness of anomaly scores. (a) The distribution fitting of VV anomaly scores of the UKB discovery group (red curve) overlaid on the distribution fitting of VV anomaly scores of the UKB replication group (blue curve). (b) The distribution fitting of WMLV anomaly scores of the UKB discovery group (red curve) overlaid on the distribution fitting of WMLV anomaly scores of the UKB replication group (blue curve). (c) The UKB discovery group subjects' FA anomaly scores (first row): The left panel shows the distribution fitting of the anomaly scores calculated using the autoencoder trained on the discovery group itself (red curve) overlaid on the distribution fitting of the anomaly scores calculated using the autoencoder trained on the replication group (blue curve). The right panel scatterplot shows these two sets of anomaly scores plotted against each other. The UKB replication group subjects' FA anomaly scores (second row):

The left panel shows the distribution fitting of the anomaly scores calculated using the autoencoder trained on the replication group itself (red curve) overlaid on the distribution fitting of the anomaly scores calculated using the autoencoder trained on the discovery group (blue curve). The right panel scatterplot shows these two sets of anomaly scores plotted against each other. **(d)** The UKB discovery group subjects' MD anomaly scores (first row): The left panel shows the distribution fitting of the anomaly scores calculated using the autoencoder trained on the discovery group itself (red curve) overlaid on the distribution fitting of the anomaly scores calculated using the autoencoder trained on the replication group (blue curve). The right panel scatterplot shows these two sets of anomaly scores plotted against each other. The UKB replication group subjects' MD anomaly scores (second row): The left panel shows the distribution fitting of the anomaly scores calculated using the autoencoder trained on the replication group itself (red curve) overlaid on the distribution fitting of the anomaly scores calculated using the autoencoder trained on the discovery group (blue curve). The right panel scatterplot shows these two sets of anomaly scores plotted against each other. **(e)** The UKB discovery group subjects' CTh anomaly scores (first two panels): The first panel shows the distribution fitting of the anomaly scores calculated using the autoencoder trained on the discovery group itself (red curve) overlaid on the distribution fitting of the anomaly scores calculated using the autoencoder trained on the replication group (blue curve). The second panel scatterplot shows these two sets of anomaly scores plotted against each other. The UKB replication group subjects' CTh anomaly scores (last two panels): The third panel shows the distribution fitting of the anomaly scores calculated using the autoencoder trained on the replication group itself (red curve) overlaid on the distribution fitting of the anomaly scores calculated using the autoencoder trained on the discovery group (blue curve). The fourth panel scatterplot shows these two sets of anomaly scores plotted against each other.

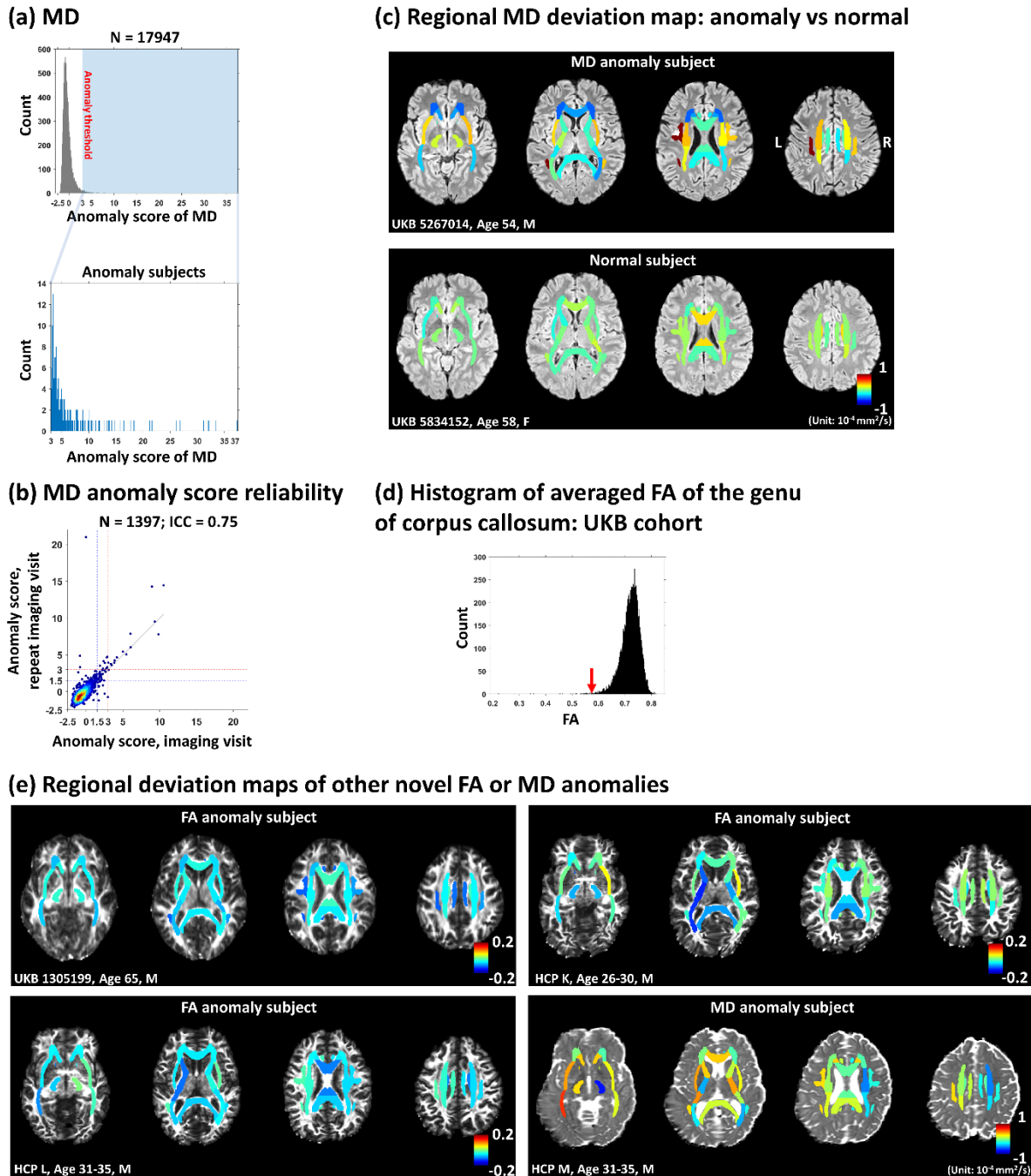


**Fig. S3.** Additional information on anomaly detection using white matter-based imaging phenotypes. **(a)** The histogram of MD anomaly scores in the UKB discovery group. The zoom panel on the second row shows the histograms of anomaly subjects (anomaly score > 3). **(b)** Long-term test-retest reliability of MD anomaly scores. In the scatterplot, each subject's anomaly score of the initial imaging visit (aka "test"; year 2014+) is plotted against the anomaly score of the first repeat imaging visit (aka "retest"; year 2019+). The UKB subjects that had both test and retest data available are shown in the scatterplot. ICC: intraclass correlation between anomaly scores of the two visits. Red dashed line: anomaly threshold (anomaly score = 3). **(c)** Regional MD deviation maps (overlaid on T2 FLAIR images) of an example of an MD anomaly subject (first row, anomaly score = 4.2) and an example of a normal MD subject (second row,

anomaly score = -1.3). An MD deviation map visualizes how the MD values in a subject deviate from the autoencoder-predicted MD values. **(d)** The histogram of averaged FA of the genu of corpus callosum in the UKB discovery group. The red arrow points to the bin for the novel FA anomaly subject reported in the right panel of Fig. 5d (UKB 1229266). **(e)** Regional deviation maps (overlaid on FA or MD images) of other novel FA or MD anomalies. (UKB 1305199, FA anomaly score = 3.6; HCP K, FA anomaly score = 3.1; HCP L, FA anomaly score = 3.1; HCP M, MD anomaly score = 3.2). For display purposes, in deviation maps, each white matter ROI is displayed in its full size instead of only the TBSS skeleton.

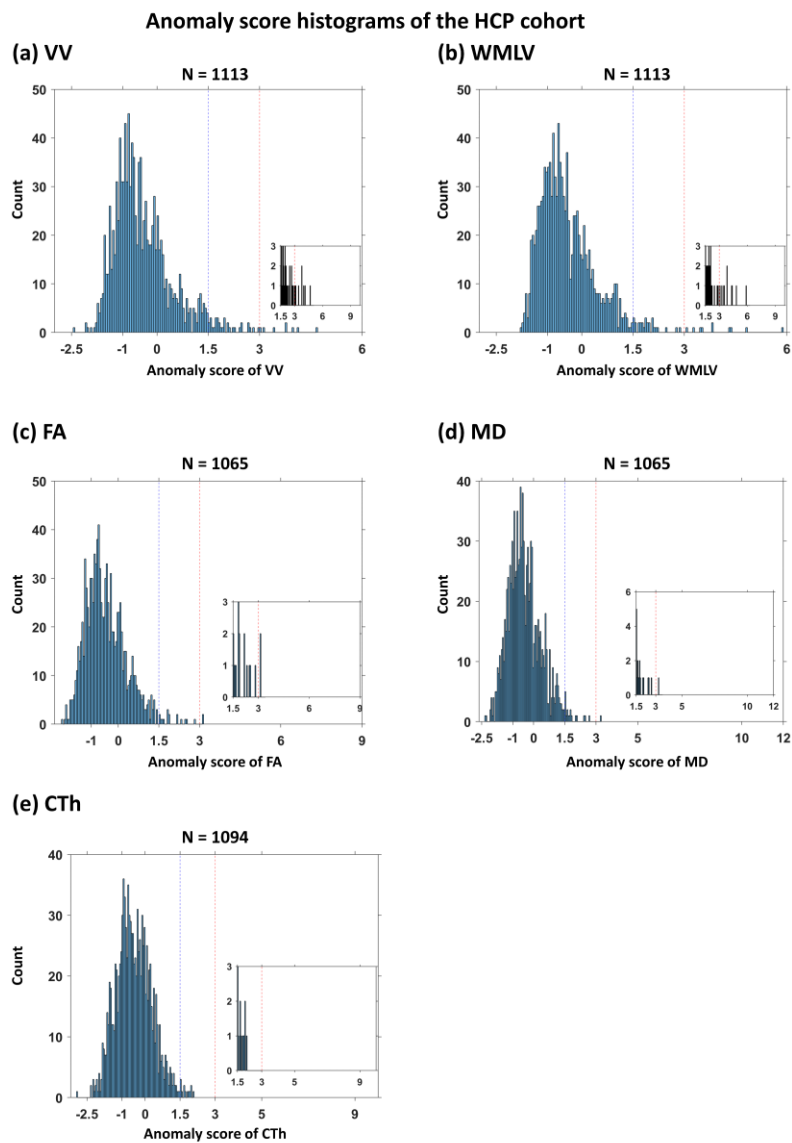
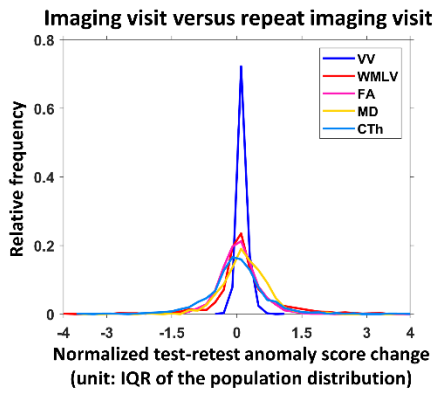


**Fig. S4.** Anomaly score histograms of the HCP subjects. (a) VV. (b) WMLV. (c) FA. (d) MD. (e) CTh. Each zoom panel on the lower right shows the histogram of the subjects whose anomaly scores were greater than 1.5.

**(a) Distribution fits of UKB anomaly score change**



**(b) Dispersions of the distributions of UKB anomaly score change**

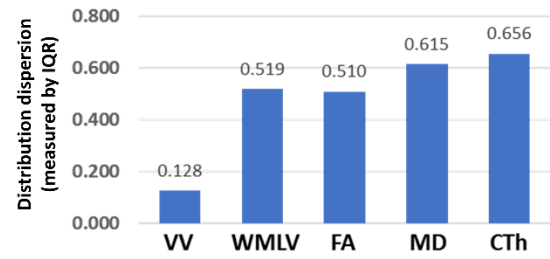
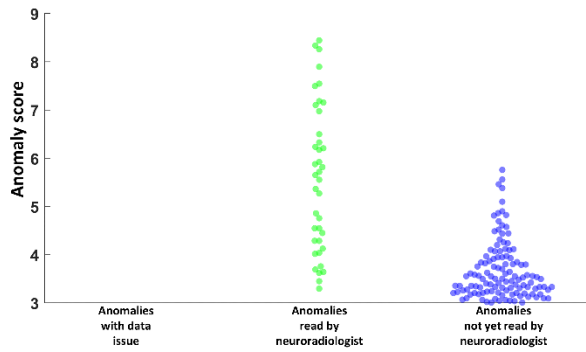
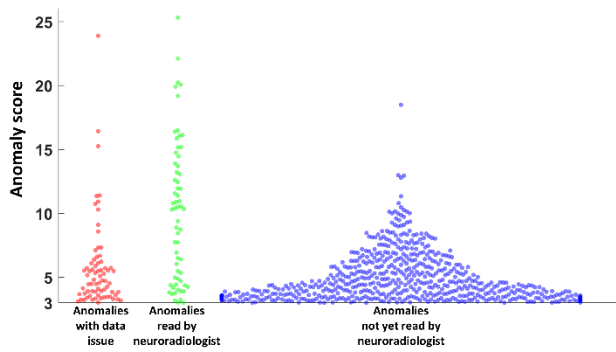


**Fig. S5.** Additional information on test-retest changes in the anomaly scores of different imaging phenotypes. **(a)** Distribution fits of UKB anomaly score change between the initial imaging visit (aka “test”; year 2014+) and the first repeat imaging visit (aka “retest”; year 2019+). **(b)** Dispersions of the distributions of UKB anomaly score change. Here dispersions were measured by the IQR values of the distributions of anomaly score change.

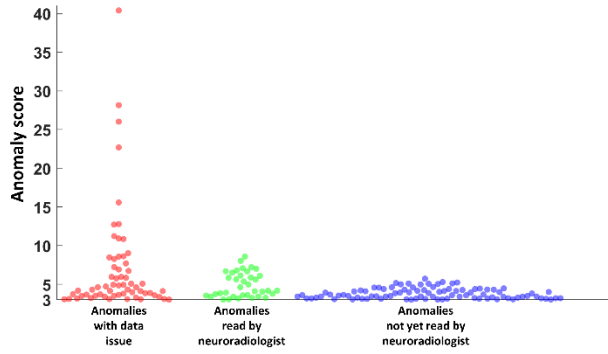
**(a) VV anomalies**



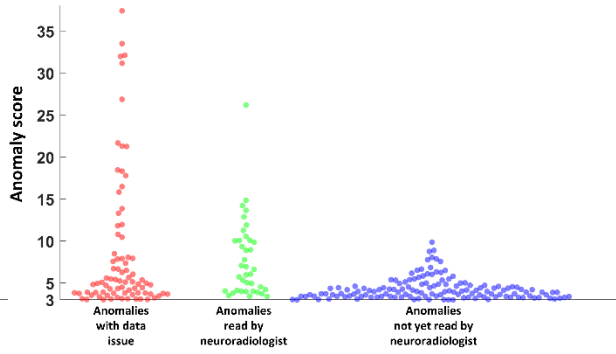
**(b) WMLV anomalies**



**(c) FA anomalies**



**(d) MD anomalies**



**(e) CTh anomalies**

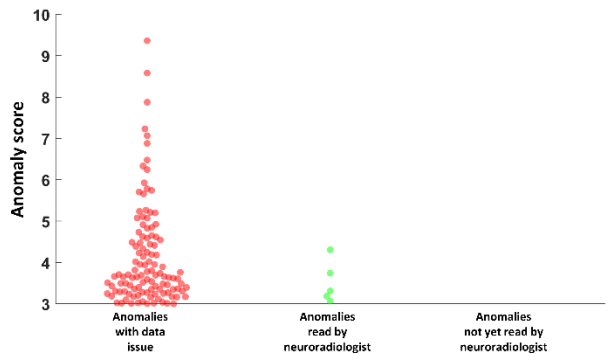
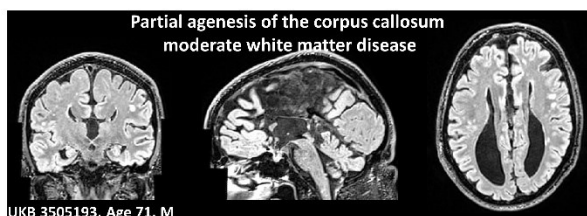
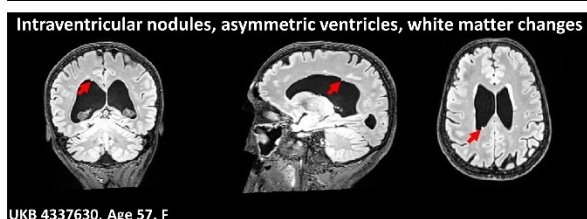
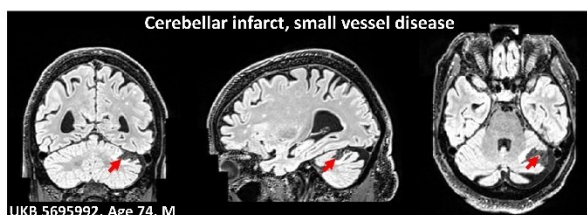
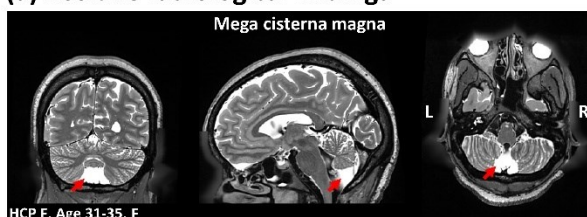
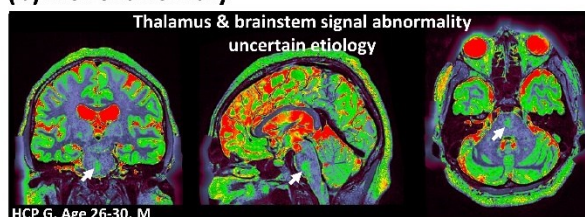


**Fig. S6.** Beeswarm plots for showing radiologically-reviewed anomaly subjects' anomaly score ranges. **(a)** VV anomalies. **(b)** WMLV anomalies. **(c)** FA anomalies. **(d)** MD anomalies. **(e)** CTh anomalies. The anomalies with data collection/processing errors are represented by red dots. A subgroup of the remaining anomalies without the errors was read by a neuroradiologist (green dots).

**(a) Positive radiological findings**



**(b) Novel anomaly**



**(c) Novel twin anomalies in the same family**

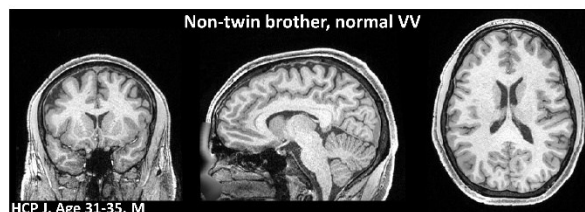
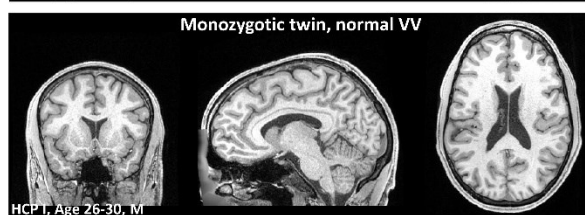
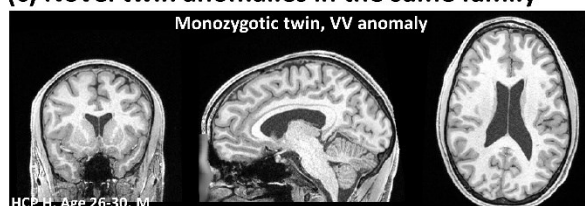
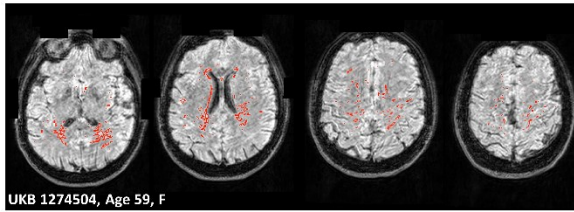
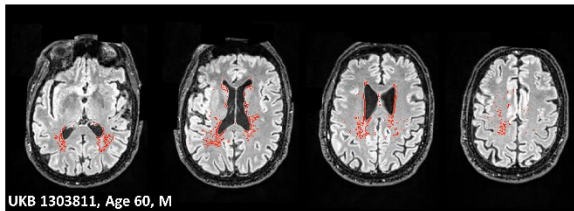


**Fig. S7.** Additional examples for the secondary screening of VV anomalies. **(a)** Structural images showing positive radiological findings in VV anomaly subjects of a mega cisterna magna (first row, anomaly score = 3.1), an infarct (second row, anomaly score = 4.0), intraventricular nodules (third row, anomaly score = 7.5), and partial agenesis of the corpus callosum (fourth row, anomaly score = 4.5). **(b)** Structural images of a novel anomaly subject with thalamus and brainstem signal abnormality of uncertain etiology (anomaly score = 4.0). **(c)** Structural images of a family (monozygotic twins and their non-twin brother). One twin (first row, anomaly scores = 3.0) was a novel VV anomaly, but the other twin (second row, anomaly score = 1.2) and their non-twin brother (third row, anomaly score = -0.4) had normal VV.

**(a) Head motion artifact in T2 FLAIR image**



**(b) Incorrect segmentation of T2 FLAIR white matter hyperintensities**



**(c) Incorrect segmentation of T1w white matter hypointensities**

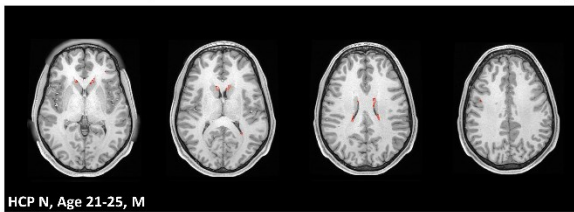
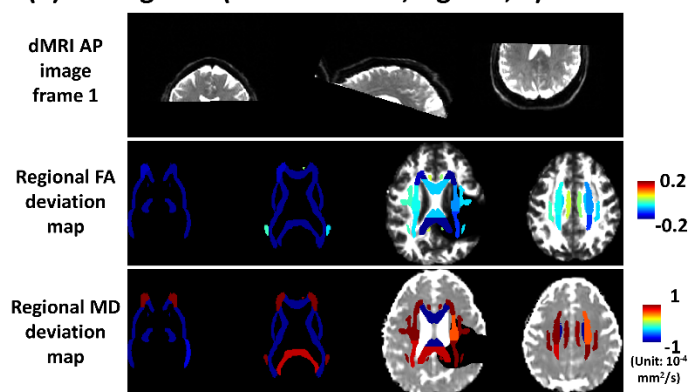
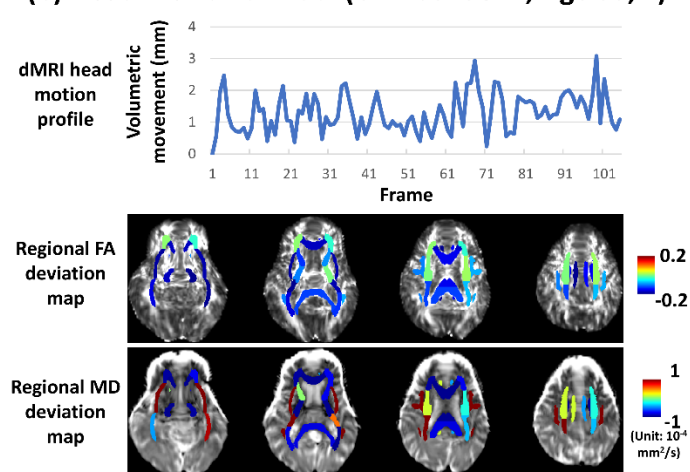


**Fig. S8.** Representative WMLV anomalies associated with data collection/processing errors. **(a)** The segmentation of white matter hyperintensities in T2 FLAIR images by BIANCA was corrupted by head motion artifact. **(b)** Incorrect segmentation of white matter hyperintensities by BIANCA in T2 FLAIR images. **(c)** Incorrect segmentation of white matter hypointensities by FreeSurfer in T1w image. The red line represents the inaccurate white matter lesion boundary segmented using BIANCA (panel a and b) or FreeSurfer (panel c).

**(a) Wrong FOV (UKB 3769716, Age 55, F)**



**(b) Head motion artifact (UKB 3579071, Age 55, F)**



**(c) Incorrect registration (UKB 3127561, Age 68, F)**

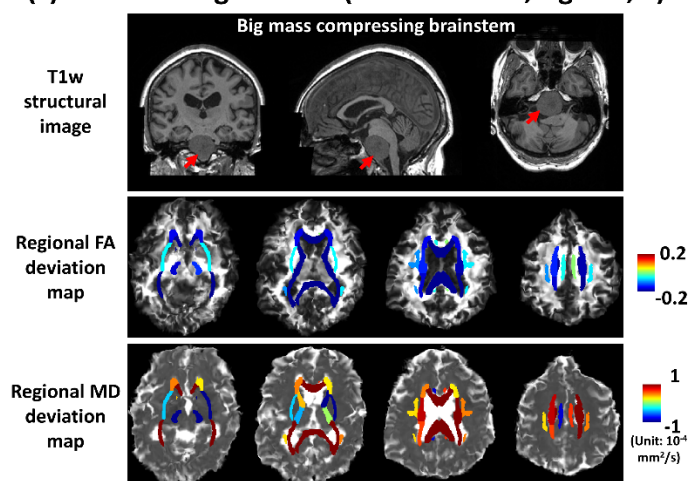
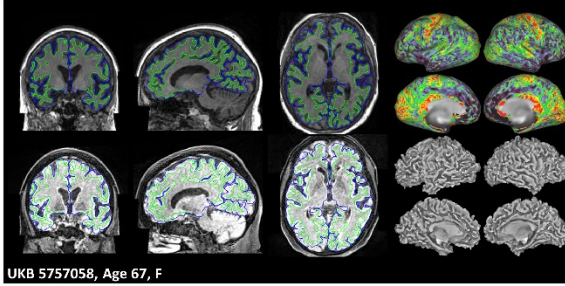


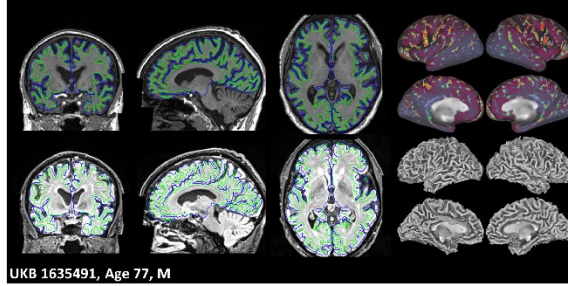
**Fig. S9.** Representative FA and MD anomalies associated with data collection/processing errors. **(a)** Wrong FOV. Missing the inferior part of the brain in dMRI images (first row) resulted in anomalously large negative FA deviations (second row) and anomalously large positive MD deviations (third row) in these missing regions. **(b)** Head motion artifact. Large volumetric movements between adjacent dMRI frames (first row) corrupted the FA image (background image in the second row) and MD image (background image in the third row). This resulted in widespread anomalously

large negative FA deviations (foreground map in the second row) and anomalously large positive MD deviations (foreground map in the third row). (c) Incorrect nonlinear registration. The registration was affected by a big mass pushing on the brainstem (first row). The FA and MD images after the registration were severely distorted (background images in the second and third rows) and this resulted in widespread anomalously large negative FA deviations (foreground map in the second row) and anomalously large positive MD deviations (foreground map in the third row). For display purposes, in these deviation maps, each white matter ROI is displayed in its full size instead of only the TBSS skeleton.

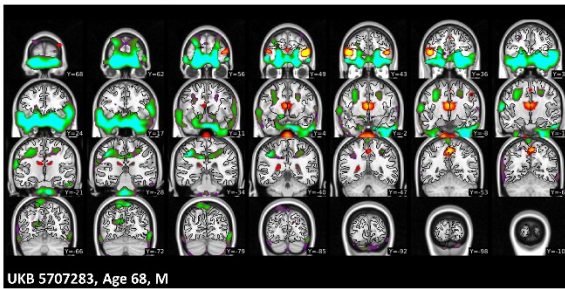
**(a) Head motion artifact**



**(b) Incorrect segmentation**



**(c) Incorrect registration**



**(d) Combination of data collection/processing errors**

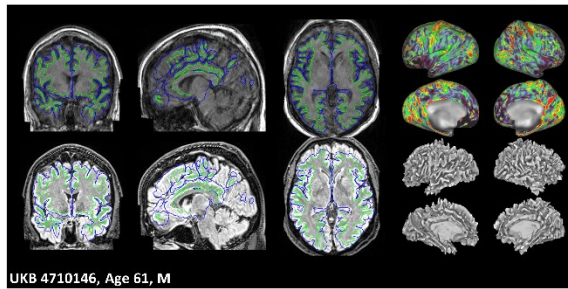
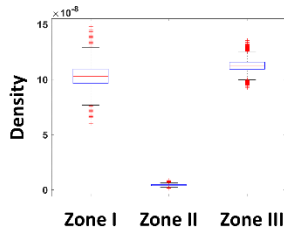
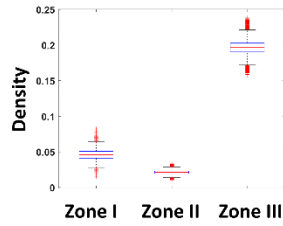


**Fig. S10.** Representative CTh anomalies associated with data collection/processing errors. These subjects are shown in the HCP structural pipeline quality control figures. **(a)** CTh anomaly subject with head motion artifact in structural images. **(b)** CTh anomaly subject with incorrect segmentation. **(c)** CTh anomaly subject with incorrect nonlinear registration of excessive volumetric deformation. **(d)** Combination of data collection and processing errors in a CTh anomaly subject.

**(a) UKB WMLV vs VV anomaly score: ANOVA of densities (100000 bootstraps)**

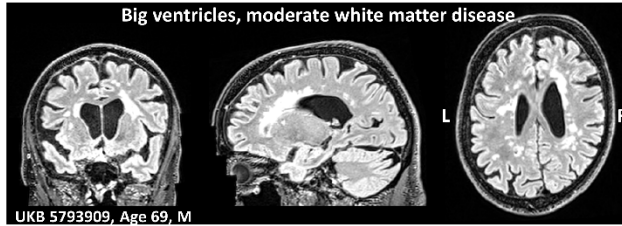


**(b) UKB WMLV vs FA anomaly score: ANOVA of densities (100000 bootstraps)**



**(c) Anomalies of more than one imaging phenotype**

**VV & WMLV anomaly**



**VV, WMLV, FA, & MD anomaly**

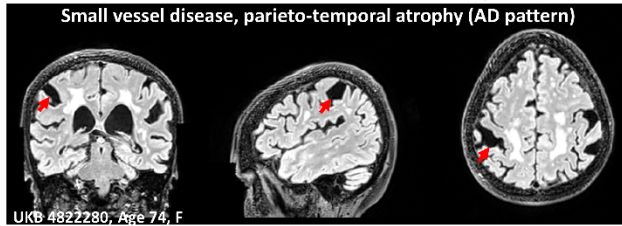


**Fig. S11.** Additional information on the relationship between anomaly scores of different imaging phenotypes. **(a)** Bootstrapping results for comparing the subject densities in Zone I, II, and III in Fig. 7b. **(b)** Bootstrapping results for comparing the subject densities in Zone I, II, and III in Fig. 7c. **(c)** Structural images showing positive radiological findings in two anomaly subjects who were anomalies in more than one imaging phenotype (anomaly scores: UKB subject 5793909, VV 4.3, WMLV 5.0; UKB subject 4822280, VV 3.8, WMLV 11.9, FA 7.0, MD 11.3).

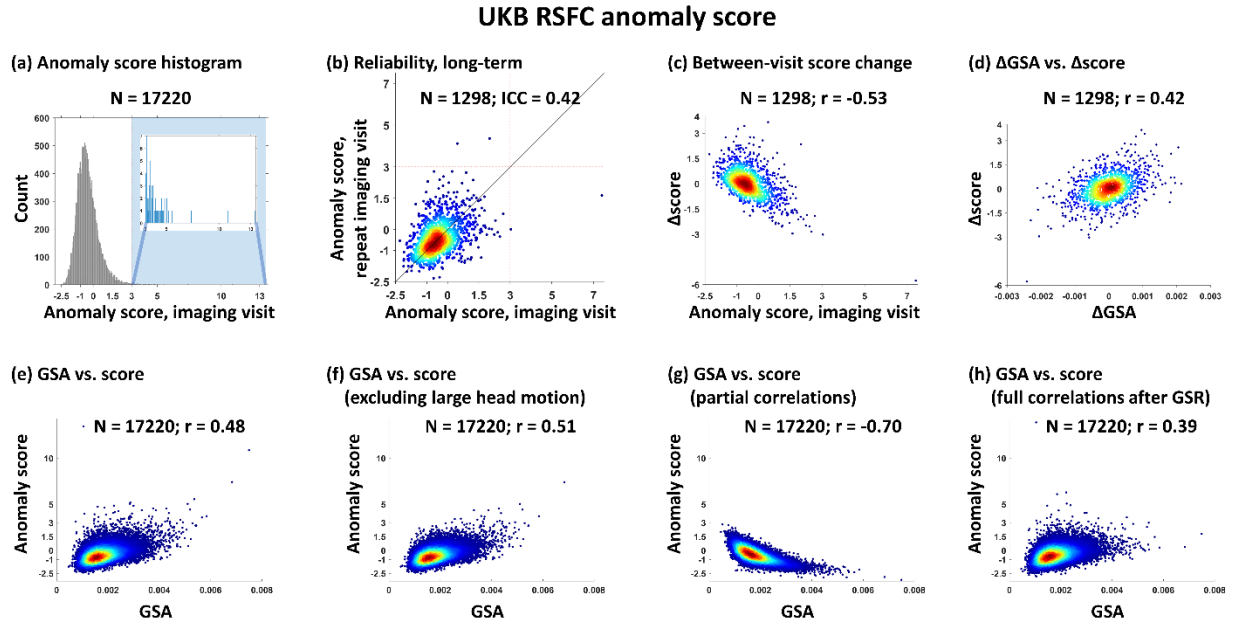


**Fig. S12.** RSFC anomaly detection in the UKB discovery group. **(a)** Anomaly score histogram. The zoom panel on the upper right shows the histogram of anomaly subjects (anomaly score > 3). **(b)** Long-term reliability of RSFC anomaly scores. Each subject's anomaly score of the initial imaging visit (aka "test"; year 2014+) is plotted against the anomaly score of the first repeat imaging visit (aka "retest"; year 2019+). Red dashed line: anomaly threshold (anomaly score = 3). **(c)** The scatterplot of RSFC anomaly score in the initial imaging visit versus between-visit anomaly score change ( $\Delta$ score = retest visit score - test visit score). **(d)** The scatterplot of between-visit global signal amplitude (GSA) change versus between-visit RSFC anomaly score change. For (b), (c), and (d), only the UKB subjects that had both test and retest data available are shown in these scatterplots. **(e)** The scatterplot of GSA versus RSFC anomaly score (RSFC calculated using full correlations). **(f)** The scatterplot of GSA versus RSFC anomaly score (RSFC calculated using full correlations) after excluding the subjects with large head motion. **(g)** The scatterplot of GSA versus RSFC anomaly score (RSFC calculated using partial correlations). **(h)** The scatterplot of GSA versus RSFC anomaly score (RSFC calculated using full correlations after global signal regression [GSR]).

### HCP RSFC anomaly score

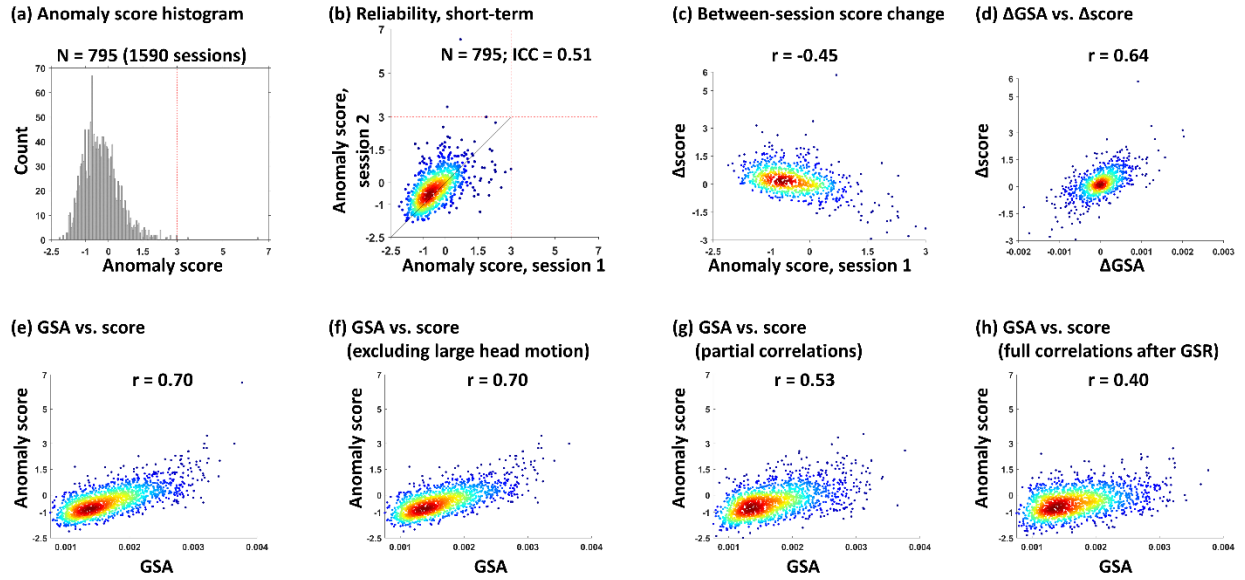


**Fig. S13.** RSFC anomaly detection in the HCP cohort. **(a)** Anomaly score histogram. Each HCP subject had two rsfMRI sessions (Day 1 session and Day 2 session). Each session was individually assigned with an anomaly score, both included in this histogram. **(b)** Short-term reliability of RSFC anomaly scores. Each subject's anomaly score of Day 1 session is plotted against the anomaly score of Day 2 session. Red dashed line: anomaly threshold (anomaly score = 3). **(c)** The scatterplot of RSFC anomaly score in Day 1 session versus between-session anomaly score change ( $\Delta$ score = Day 2 session score - Day 1 session score). **(d)** The scatterplot of between-session global signal amplitude (GSA) change versus between-session RSFC anomaly score change. **(e)** The scatterplot of GSA versus RSFC anomaly score (RSFC calculated using full correlations). **(f)** The scatterplot of GSA versus RSFC anomaly score (RSFC calculated using full correlations) after excluding the sessions with large head motion. **(g)** The scatterplot of GSA versus RSFC anomaly score (RSFC calculated using partial correlations). **(h)** The scatterplot of GSA versus RSFC anomaly score (RSFC calculated using full correlations after global signal regression [GSR]).

**(a) UKB anomaly scores versus confounding factors**   **(b) HCP anomaly scores versus confounding factors**

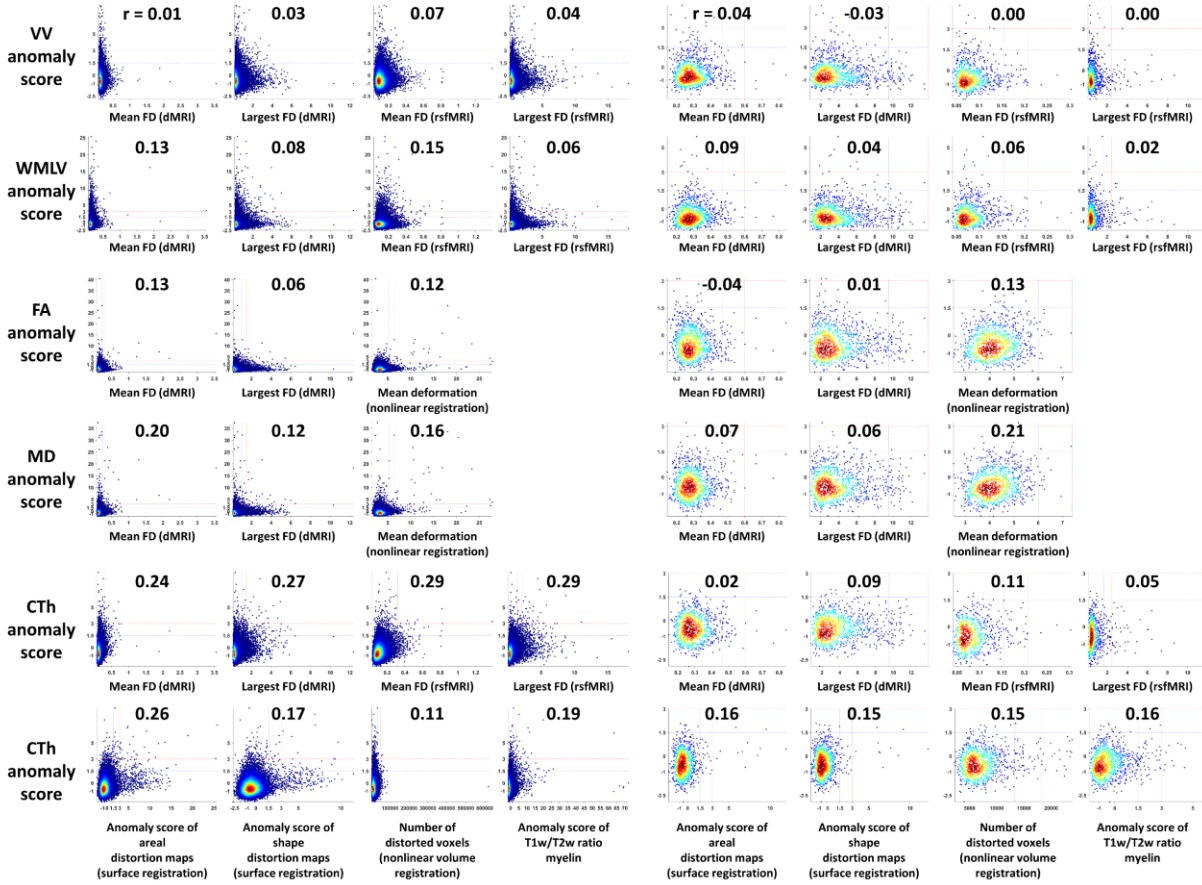


**Fig. S14.** Anomaly scores versus confounding factors. **(a)** UKB discovery group subjects. **(b)** HCP subjects. Each small panel shows a scatterplot between the anomaly score of an imaging phenotype (vertical axis) versus a confounding factor (horizontal axis), and the Pearson correlation between the two quantities is shown above each scatterplot. FD: framewise displacement (unit: mm).

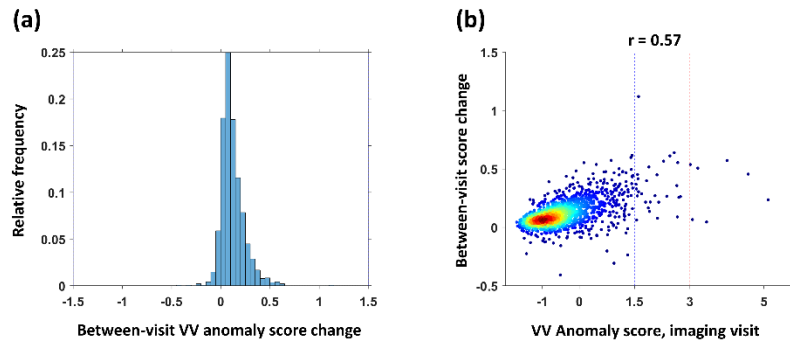


**Fig. S15.** VV anomaly score was significantly higher in the repeat imaging visit. **(a)** The histogram of between-visit VV anomaly score change. Here, between-visit score change = retest visit score - test visit score. **(b)** The scatterplot of VV anomaly score in the initial imaging visit versus between-visit anomaly score change.

**Table S1.** Summary of the demographic information of the UKB discovery group and HCP subjects used in this study.

Modality	UKB discovery group									HCP					
	Number of subjects	Gender		Age						Number of subjects	Gender		Age		
		M	F	40-49	50-59	60-69	70-79	80-89	mean $\pm$ SD		M	F	20-29	30-39	mean $\pm$ SD
T1w	19411	9172	10239	782	6046	8791	3789	3	62.5 $\pm$ 7.5	1113	507	606	623	490	28.8 $\pm$ 3.7
T2w	18467	8701	9766	716	5767	8375	3606	3	62.5 $\pm$ 7.4	1094	496	598	609	485	28.8 $\pm$ 3.7
dMRI	17947	8430	9517	694	5631	8134	3485	3	62.5 $\pm$ 7.4	1065	490	575	601	464	28.7 $\pm$ 3.7
rsfMRI	17221	8074	9147	662	5412	7789	3355	3	62.5 $\pm$ 7.4	795	388	407	477	318	28.4 $\pm$ 3.7

**Table S2.** Twenty-seven white matter ROIs from the John Hopkins University white matter atlas (Mori et al., 2008) were used in the anomaly detection of FA and MD.

ROI name
Genu of corpus callosum
Body of corpus callosum
Splenium of corpus callosum
Right cerebral peduncle
Left cerebral peduncle
Right anterior limb of internal capsule
Left anterior limb of internal capsule
Right posterior limb of internal capsule
Left posterior limb of internal capsule
Right retrolenticular part of internal capsule
Left retrolenticular part of internal capsule
Right anterior corona radiata
Left anterior corona radiata
Right superior corona radiata
Left superior corona radiata
Right posterior corona radiata
Left posterior corona radiata
Right posterior thalamic radiation (include optic radiation)
Left posterior thalamic radiation (include optic radiation)
Right sagittal stratum (include inferior longitudinal fasciculus and inferior fronto-occipital fasciculus)
Left sagittal stratum (include inferior longitudinal fasciculus and inferior fronto-occipital fasciculus)
Right external capsule
Left external capsule
Right cingulum (cingulate gyrus)
Left cingulum (cingulate gyrus)
Right superior longitudinal fasciculus
Left superior longitudinal fasciculus

**Table S3.** Summary of the demographic information of the UKB replication group used in this study.

Number of subjects	Gender		Age					
	M	F	40- 49	50- 59	60- 69	70- 79	80- 89	mean $\pm$ SD
19350	9005	10345	104	5164	8164	5798	120	64.7 $\pm$ 7.4

**Table S4.** Summary of anomaly subjects in the HCP cohort.

Phenotype		VV	WMLV	FA	MD	CTh
Number of Subjects		1113	1113	1065	1065	1094
Skewness		1.50	1.85	0.92	0.68	0.33
Kurtosis		6.64	9.33	4.42	3.71	3.14
Number of Anomalies		8 (0.7%)	10 (0.9%)	2 (0.2%)	1 (0.1%)	0 (0%)
Anomalies w/o data issue		8	3	2	1	
Anomalies read by neuroradiologist		8	3	2	1	
Summary of radiological review results	Large ventricles	8				
	White matter lesions		2			
	Mass					
	Cyst	1				
	Infarct					
	Encephalo-malacia					
	Prominent sulci					
	Other findings	2	1			
	Normal			2	1	

Note: Empty entries are zeros.